Volume 253, No. 23, 30 September 2007 ISSN 0169-4332

ELSEVIER

applied
surface science

A journal devoted to applied physics
and chemistry of surfaces and interfaces

Volume 253, No. 23, pp. 9047–9290

30 September 2007

Available online at www.sciencedirect.com
ScienceDirect
http://www.elsevier.com/locate/apsusc

Available online at www.sciencedirect.com
ScienceDirect
Applied Surface Science 253 (2007) 9221–9227
applied surface science
www.elsevier.com/locate/apsusc

Dissociative adsorption and thermal evolution of dichloroethylenes on Ni(1 0 0)

S.H. Xu [1], X. Yang [2], Z.H. He, K.T. Leung *

Department of Chemistry, University of Waterloo, Waterloo, Ontario N2L 3G1, Canada

Received 18 December 2006; accepted 23 May 2007
Available online 2 June 2007

Abstract

The room temperature (RT) adsorption and thermal evolution of *cis*- and *trans*-dichloroethylene (DCE) and their structural isomer, *iso*-DCE, on Ni(1 0 0) have been studied by vibrational electron energy loss spectroscopy (EELS), Auger electron spectroscopy (AES) and thermal desorption spectrometry (TDS). For RT adsorption, both *cis*- and *trans*-DCE exhibit very similar EELS features that are different from those found for *iso*-DCE. These differences indicate the formation of different fragments upon RT adsorption. In particular, the primary adspecies for *cis*- and *trans*-DCE are ethane-1,1,2,2-tetrayl ($\mathrm{H\ddot{C}{-}\ddot{C}H}$) and acetylide-like ($\cdot\,\mathrm{\dot{C}=\dot{C}H} \leftrightarrow \cdot\,\mathrm{\ddot{C}-\ddot{C}H}$) adspecies along with a small amount of chlorovinyl adspecies, while ethylylidyne ($\cdot\,\mathrm{\ddot{C}-\dot{C}H_2}$) is the more plausible adspecies for *iso*-DCE. The differences in the adstructures upon dissociative adsorption at RT underline the important isomeric effects. Furthermore, both AES and TDS results for all three DCE isomers show that most of the Cl atoms produced by dechlorination remain on the surface and its surface concentration remains unchanged upon annealing the samples above 500 K. Upon further annealing to 550 K, the EELS spectra of all three isomers exhibit a broad feature near 1600 $\mathrm{cm^{-1}}$, which suggests the formation of carbon clusters on the surface. The presence of surface Cl atoms therefore appears to prevent the C–C bond cleavage during thermal evolution of the adspecies on Ni(1 0 0).

Keywords: Dissociative adsorption; Dichloroethylenes; Ni(1 0 0)

1. Introduction

Nickel is a particularly important catalyst used in a variety of chemical reactions, including hydrogenation, dehydrogenation, isomerization and oxidation. The low cost of Ni has made it an attractive alternative to other precious metals (Pd and Pt) to be used as the substrate to further exploit catalytic surface reactions. The study of molecular adsorption at room temperature (RT) offers insights into the mechanisms of surface chemical reactions that are of interest to industrial processes. Numerous studies on the adsorption of such benchmark hydrocarbon molecules as acetylene, ethylene and benzene on the (1 0 0), (1 1 1) and (1 1 0) surfaces of Ni have been reported [1–7]. In comparison with other metal surfaces, different interactions between these unsaturated hydrocarbon adsorbates (acetylene, ethylene, benzene) and the Ni substrate are found. In particular, the rate of hydrogenation over metal catalysts generally follows the order: Pd > Pt > Ni, while the rate of isomerization tends to observe a different order: Pd > Ni > Pt. Furthermore, there are often notable differences in the surface chemistry of the same adsorbate on the same substrate prepared by different procedures. For example, notable differences indicative of the reactive nature of the Ni(1 1 0) substrate are found in the EELS spectra for benzene as-deposited at RT and for benzene deposited at 110 K followed by annealing to RT [8].

The study of the transformation of harmful chlorinated hydrocarbons on metal surfaces into safe species is also of special interest to environmental studies. These studies can be useful not only to understand the (hydro)dechlorination process at the molecular level, but also to evaluate the efficiency and mechanisms of the catalysts involved. Among the various

---

* Corresponding author. Tel.: +1 519 888 4567x35826; fax: +1 519 746 0435.
E-mail address: tong@uwaterloo.ca (K.T. Leung).
URL: http://www.leung.uwaterloo.ca

[1] Present address: Alberta Centre for Surface Engineering and Science, University of Alberta, Edmonton, Alberta T6G 2G6, Canada.

[2] Present address: Faculty of Graduate Studies and Research, Saint Mary's University, Halifax, Nova Scotia B3H 3C3, Canada.

0169-4332/$ – see front matter © 2007 Elsevier B.V. All rights reserved.
doi:10.1016/j.apsusc.2007.05.052

chlorinated hydrocarbons, the geometrical isomers (*cis* and *trans*) and its structural isomer (*iso*) homolog of dichloroethylene (DCE) on metal surfaces offer simple model systems for investigating the surface dechlorination process. The early studies of chlorinated ethylenes on metal surfaces have largely focussed on multilayer (physi-)adsorption near the liquid-nitrogen temperature and chemisorption behaviour upon annealing to RT. In particular, using vibrational electron energy loss spectroscopy (EELS) and thermal desorption spectrometry (TDS), Grassian and Pimental showed that *cis*- and *trans*-DCE form di-σ bonds with Pt(1 1 1) in staggered, alkane-like geometries upon monolayer and submonolayer adsorption at 110 K, and undergo dechlorination above 200 K producing a vinylene or ethene-1,2-diyl ($H\dot{C}{=}\dot{C}H$) adspecies [9].[3] When the sample was further annealed to a higher temperature, recombinative desorption of HCl from dissociated Cl atoms at 460 K followed by further decomposition of the resulting adspecies at a higher temperature (leaving only C behind on the surface) were observed. On the other hand, Cassuto et al. concluded from their near-edge X-ray absorption fine-structure spectroscopy (NEXAFS) and ultraviolet photoemission spectroscopy (UPS) studies that on Pt(1 1 1) and Pt(1 1 0), DCE (*cis*, *trans* and *iso* isomers), trichloroethylene and perchloroethylene are weakly bonded at 95 K (with the molecular plane parallel to the surface) and they could be desorbed molecularly above 120 K–130 K [10].

Similar experimental results have also been observed for chlorinated ethylenes on Cu(1 0 0) [11] and Cu(1 1 0) [12,13] surfaces. In particular, Yang et al. studied the chemical bonding and reactions of a series of chlorinated ethylenes (including monochloroethylene, *cis*- and *trans*-DCE, and trichloroethylene) on Cu(1 0 0) using TDS and NEXAFS technique [11], and they suggested that molecular adsorption of these chloroethylenes at 95 K could involve π-bonding interaction with the Cu surface. With the exception of monochloroethylene that was found to desorb molecularly upon annealing, enhanced dechlorination with increasing Cl content in the adsorbates was observed for the heavier chloroethylenes, and the resulting dissociated hydrocarbon product (acetylene) could lead to benzene evolution in the case of *cis*- and *trans*-DCE, and trichloroethylene [11]. However, on the basis of their EELS data, Jugnet et al. proposed a di-σ bonded adstructure for *trans*-DCE chemisorbed on Cu(1 1 0) at 135 K, which could evolve into acetylene-like adspecies by Cl dissociation upon annealing to ~200 K and to benzene at a higher temperature (>350 K) [12]. The formation of benzene could also be observed by direct adsorption of *trans*-DCE at RT [12].

The adsorption of DCE on Pd(1 0 0) and Pd(1 1 0) surfaces was found to be more complicated [14,15]. Bloxham et al. showed that the adsorption, decomposition and product evolution pathways of *trans*-DCE on Pd(1 1 0) depend on both the reactant uptake and substrate temperature [15]. These studies generally showed that the thermal evolution behaviours on Pt, Cu, and Pd surfaces for the two geometrical isomers, *cis*- and *trans*-DCE, are similar to each other. Although there are relatively more studies about the adsorption of *cis*- and *trans*-DCE on these metal surfaces, very few studies about *iso*-DCE on single-crystal metal surfaces have been reported in the literature. In recent studies of *cis*-DCE and *iso*-DCE on Pd(1 1 1) [16,17], Land and coworkers showed that ethylidyne ($\cdot\ddot{C}-CH_3$) was formed on the surface upon annealing *cis*-DCE adsorbed at 130 K–220 K or *iso*-DCE adsorbed at 100 K to <300 K. Desorption products: H_2 and HCl were also observed above 370 K for *cis*-DCE and 425 K for *iso*-DCE. Land and coworkers further proposed 2-chlorovinyl and vinylidene-like $[\cdot\dot{C}=CH_2\,(\text{vinylidene})\leftrightarrow\cdot\ddot{C}-\dot{C}H_2\,(\text{ethylilydyne})]$ adspecies as plausible intermediates for *cis*-DCE and *iso*-DCE, respectively, on Pd(1 1 1) [16,17].

Differences have also been found when the same DCE molecule adsorbed on different metal surfaces. For example, recombinative Cl_2 or HCl desorption was not observed on Cu(1 1 0) [12,13] by using TDS, in contrast to that found on the Pt(1 1 1) [9], Pt(1 1 0) [10] and Pd(1 1 1) surfaces [16,17]. The arrangements of the two Cl atoms in different relative positions in DCE therefore provide interesting possible adstructures to investigate isomeric effects. To our knowledge, there has been no experimental result reported on the adsorption of DCE on single-crystal Ni surfaces. In the present work, we follow the RT adsorption and thermal evolution of the three DCE isomers on Ni(1 0 0) by using vibrational EELS, TDS and AES, and compare the corresponding surface processes of *cis*- and *trans*-DCE with those of its structural isomer, *iso*-DCE.

2. Experimental details

All the experiments in the present work were conducted in a home-built ultrahigh vacuum (UHV) system, with a base pressure better than 1×10^{-10} Torr. The UHV system was equipped with an ion-sputtering gun, a four-grid retarding-field optics for reverse-view low energy electron diffraction (LEED) and AES studies, a differentially pumped 1 amu–300 amu quadrupole mass spectrometer for TDS experiments, and a home-built multi-technique electron spectrometer for both electronic and vibrational EELS measurements. Details of our UHV system and EELS spectrometer have been described in our earlier work [18]. All the vibrational EELS experiments were performed using a specular reflection geometry (45° from the surface normal) with an impact energy of 5 eV. A routine energy resolution of 150 cm^{-1} full-width at half-maximum (FWHM) could be achieved, with a typical count rate of 100,000–300,000 counts/s for the elastic peak.

The single-side polished Ni(1 0 0) substrate (10 mm in diameter and 1 mm thick) with a stated purity of 99.995% and an accuracy of ±1° from the (1 0 0) plane was purchased from Accumet Materials. The substrate was mechanically fastened onto the Ta sample plate by spot-welding with Ta strips (0.5 mm thick). The Ni crystal was cleaned by repeated cycles of Ar^+ sputtering and annealing to 1000 K until a sharp 1 × 1 LEED pattern was obtained. The surface cleanliness of the substrate was further confirmed by a featureless EELS

---

[3] We use "·" to denote an unpaired electron on the adsorbate available for bonding with a substrate atom.

spectrum and by AES that showed no C, S and O signal. Sample annealing was achieved by electron bombardment from a heated W filament at the backside of the Ni sample. The temperature of the substrate was measured by a K-type thermocouple (mechanically fastened to the front side of the sample) with an absolute accuracy of ±20 K. Because the presence of residual CO (and CO_2) in our UHV chamber could easily lead to contamination on the relatively reactive, clean Ni surface (as indicated by a strong C=O stretching mode near 1800 cm^{-1} in the EELS spectrum), we used circulated liquid nitrogen to reduce the amount of time required to cool the sample back to RT in order to minimize possible surface contamination before sample dosing.

The liquid samples: *iso*-DCE (99% purity), *cis*-DCE (98%), and *trans*-DCE (98% purity) were purchased from Sigma–Aldrich and degassed by several freeze–pump–thaw cycles prior to use. No discernible impurities could be found in the respective cracking patterns of the chemicals during sample dosing. The exposure in units of Langmuir ($1\ L = 1 \times 10^{-6}$ Torr s) was controlled by backfilling the UHV chamber to a predetermined chamber pressure (as measured by an uncalibrated ionization gauge) for an appropriate period of time by using a variable leak valve. All the exposures were performed at RT and a saturation exposure was used unless stated otherwise.

3. Results and discussion

3.1. Adsorption at room temperature

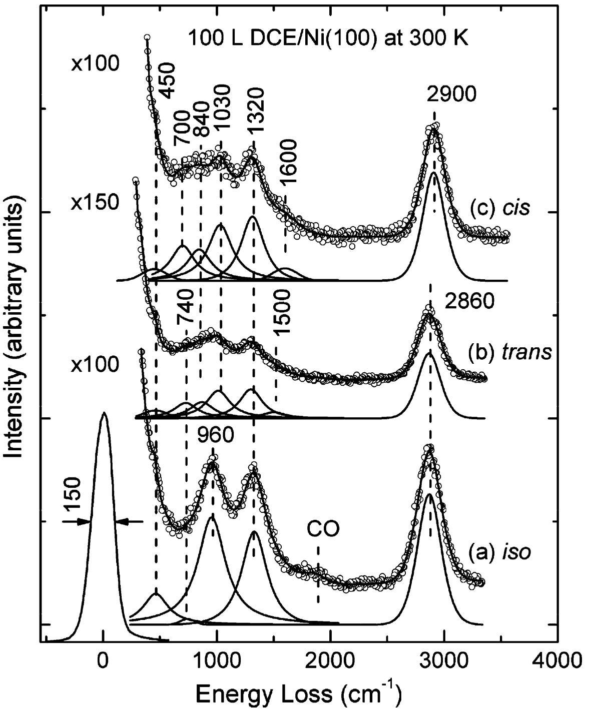

Fig. 1. Electron energy loss spectra of 100 L (a) *iso*-dichloroethylene (DCE), (b) *trans*-DCE, and (c) *cis*-DCE exposed to Ni(1 0 0) at room temperature. A nonlinear least-square curve fitting procedure using a mixture of Gaussian–Lorentzian lineshapes is used to deconvolute the underlying vibrational features.

Fig. 1 compares the vibrational EELS spectra of three DCE isomers exposed to Ni(1 0 0) at RT. Because the instrumental energy resolution of our home-built EELS spectrometer is typically limited to 150 cm^{-1} FWHM after sample dosing, possible close-lying overlapping EELS features of dissociated surface species along with some weak features in the background cannot be easily identified. Despite this difficulty to definitively identify the weak features, particularly those near the elastic peak such as the Ni–Cl stretch (at ~340 cm^{-1}) [19] and Ni–C symmetric stretch (at ~430 cm^{-1}) [1], several strong features are clearly observed in the spectra. In order to isolate the more obscured vibrational features, a nonlinear-least-square curve-fitting procedure involving a mixture of Gaussian–Lorentzian lineshapes (with an approximate mixing ratio of 1:1) has been applied to the spectra. Given the comparable FWHM values obtained for the fitted peaks (180–220 cm^{-1}) and the very flat residuals, there are excellent agreement between the fitted spectra and the experimental data (as shown in Fig. 1). Evidently, all three DCE isomers exhibit generally similar EELS spectra, with better-defined features found for *iso*-DCE (Fig. 1). In particular, the three prominent EELS features located at 960–1030 cm^{-1}, 1300–1320 cm^{-1} and 2860–2900 cm^{-1} are observed for all three DCE isomers. Although the feature near 2900 cm^{-1} can be readily attributed to the C–H stretching mode in CH or CH_2 containing surface species, the assignments of the features near 1000 cm^{-1} and 1320 cm^{-1} are not so straightforward, because various CH_x bending and C–C stretching modes are generally found in these regions [1]. As discussed below, the small but discernible changes of these features can however be used to help identify the surface adspecies. It should be noted that the prominent features at 960 and 1320 cm^{-1} are found to be nearly as intense as the feature at 2860 cm^{-1} for *iso*-DCE (Fig. 1a) while those of the corresponding features for *cis*-DCE (Fig. 1c) and *trans*-DCE (Fig. 1b) are discernibly weaker than their respective features near 2900 cm^{-1}. The differences in the relative intensities of these lower-lying features suggest possible additional contributions from adspecies found for *iso*-DCE but not for *cis*-DCE and *trans*-DCE.

In addition to these main features, there are several weaker features shown in Fig. 1. In particular, the weak shoulder at 450 cm^{-1} found for all three isomers can be assigned to the Ni–C stretching mode, in good accord with similar features found near 430 cm^{-1} for both acetylene and ethylene on Ni surfaces [1]. Similar wavenumber values for the metal-to-C stretching modes have also been reported for *trans*-DCE on Cu(1 1 0) [12] (425 cm^{-1}) and *cis*-DCE (445 cm^{-1}) and *trans*-DCE on Pt(1 1 1) (240 cm^{-1}) [9]. Another weak shoulder at 1500–1600 cm^{-1} that is evident for both *cis*- and *trans*-DCE but not *iso*-DCE on Ni(1 0 0) (Fig. 1) can be attributed to the C=C stretching mode [1,9,20]. The valley near 700 cm^{-1} for *iso*-DCE is much deeper than that for either *cis*- or *trans*-DCE, which suggests the presence of weak features near 700 cm^{-1} in the latter cases (Fig. 1). Our fitting procedure shows that there could be two peaks located at 700/740 cm^{-1} and 840 cm^{-1} for *cis*-/*trans*-DCE, while only residual intensity at 740 cm^{-1} can be isolated for *iso*-DCE.

Table 1
Comparison of the wavenumbers (cm^{-1}) and their spectral assignments of vibrational features observed for the adsorption of *iso*-, *trans*- and *cis*-dichloroethylene on Ni(1 0 0) with those for acetylene and ethylene on Ni and other metal surfaces

Mode	Dichloroethylene (this work)			Acetylenic adspecies ($H\ddot{C}{-}\ddot{C}H$)		Acetylide-like adspecies ($\cdot\dot{C}=\dot{C}H \leftrightarrow \cdot\ddot{C}-\ddot{C}H$)		Ethylylidyne ($\cdot\ddot{C}-\dot{C}H_2$)	
	iso	*trans*	*cis*	Ni(1 0 0) [1]	Ni(1 1 1) [7]	Ni(1 0 0) [1]	Ni(1 1 0) [6]	Rh(1 1 1) [23]	Pt(1 1 1) [24]
ν(Ni–C)	450	450	450	230, 435	480	–	380–465	470	–
γ(C–H)	740	740	700	730	690, 860	730	–	–	–
δ_s(C–H)	–	840	840	–	1080	820^{a}	890^{a}	–	–
δ_{as}(C–H)	960	1010	1030	970–1025	1370	–	–	–	–
ρ_w(CH$_2$)	960	–	–	–	–	–	–	990	900
ν(C–C)	1320	1300	1320	1345–1360	1220	–	1290	1145	1130
δ(CH$_2$)	1320	–	–	–	–	–	–	1405	1420
ν(C=C)	–	1500	1600	–	–	–	–	–	–
ν_s(CH$_2$)	2860	–	–	–	–	–	–	2950	2970
ν(C–H)	2860	2860	2910	2920–2950	2946	–	2990	–	–

ν, stretch; ν_s, symmetric stretch; γ, out-of-plane bend for CH; δ_s, δ_{as}, symmetric and antisymmetric in-plane bend, respectively, for CH; δ, scissoring for CH$_2$; ρ_w, wagging for CH$_2$.

[a] There is no differentiation between symmetric or asymmetric bending in the case of CCH.

In order to better assign these vibrational features and analyze the possible surface adspecies, we compare our results with the previous studies of acetylene and ethylene on Ni(1 0 0) [1,2], and CCl$_4$ on Ni(1 1 0) [19]. In particular, Chesters and Lennon showed that CCl$_4$ dissociates completely on Ni(1 1 0) at RT [19], which provides evidence for the facile C–Cl bond cleavage activated on Ni surfaces. Similarly, Cl abstraction of DCE has also been observed on Pt [9] and Pd surfaces [14–17]. It is therefore reasonable to expect similar dechlorination to take place upon RT adsorption of DCE on Ni(1 0 0). Zaera and Hall showed that dehydrogenation of acetylene and ethylene on Ni(1 0 0) also occurs near RT, but with the C–C bonds remaining intact [1,2]. Given that the bond strength for the C–Cl bond (339 kJ mol^{-1}) is generally smaller than that of C–H bonds (414 kJ mol^{-1}) [21], this thermodynamic consideration would favour dechlorination rather than dehydrogenation. We therefore believe that the dominant adspecies for RT adsorption of DCE are likely dechlorinated C$_2$-containing hydrocarbon fragments multiply bonded to the Ni(1 0 0) surface. Furthermore, Zaera and Hall also showed that acetylene chemisorbs molecularly at 90 K forming a rehybridized ‘‘acetylenic’’ or ethane-1,1,2,2-tetrayl adspecies ($H\ddot{C}{-}\ddot{C}H$) on Ni(1 0 0) [1,2]. The ethane-1,1,2,2-tetrayl adspecies was found to be stable up to 270 K, above which dehydrogenation took place to form ‘‘CCH residues’’. Similarly, annealing ethylene deposited at 90 K on Ni(1 0 0) to 275 K was also found to produce similar acetylenic adspecies [1,2]. The main EELS features for this acetylenic adspecies reported by Zaera and Hall are located at ~730 cm^{-1} (out-of-plane CH bending), 980 cm^{-1} (in-plane CH bending), 1340 cm^{-1} (C–C stretch), and 2925–2950 cm^{-1} (C–H stretch). Above 325 K, an additional EELS feature near 820 cm^{-1} was observed and used as evidence for the formation of the acetylide-like or CCH adspecies [1,2]. It should be noted that the adsorption configurations for the acetylide-like adspecies could in general involve different bonding to one or more substrate atoms, including ethynyl ($\dot{C}{\equiv}CH$), ethene-1,1,2-triyl ($\cdot\dot{C}=\dot{C}H$), and ethane-1,1,1,2,2-pentayl ($\cdot\ddot{C}-\ddot{C}H$) adspecies. Since the previous (and the present) studies have shown no evidence of the C≡C triple bond [1,2], only the resonance configurations of the multi-dentate $\cdot\dot{C}=\dot{C}H$ and $\cdot\ddot{C}-\ddot{C}H$ adspecies are considered in the present work.

Table 1 compares the wavenumbers of the vibrational features for the aforementioned rehybridized acetylenic and acetylide-like adspeices [1,2] with those of the corresponding vibrational features for the three DCE isomers on Ni(1 0 0) observed in the present work. Evidently, the energy positions of the EELS features for the *cis*- and *trans*-DCE isomers at 700–740 cm^{-1}, 840 cm^{-1}, 1010–1030 cm^{-1}, 1300–1320 cm^{-1} and 2860–2910 cm^{-1} shown in Fig. 1 are found to be similar to those of acetylenic ($H\ddot{C}-\ddot{C}H$) and acetylide-like ($\cdot\dot{C}=\dot{C}H \leftrightarrow \cdot\ddot{C}-\ddot{C}H$) adspecies for acetylene and ethylene adsorption on Ni(1 0 0) [1,2], despite the differences in their respective relative intensities. These similarities therefore suggest that similar acetylenic and acetylide-like adspecies are plausible for the RT adsorption of *cis*- and *trans*-DCE on Ni(1 0 0). The differences in the relative intensities of the corresponding features may be due to the differences in the relative surface concentrations of acetylenic and acetylide-like adspecies produced from the respective adsorbates. Furthermore, the presence of the weak C=C stretching mode at 1600 cm^{-1} for *cis*-DCE and 1500 cm^{-1} for *trans*-DCE not found for the acetylene and ethylene cases [1,2] suggests the formation of a small amount of 2-chlorovinyl ($H\dot{C}=C{<}^{H}_{Cl}$) adspecies likely by single dechlorination. The formation of similar 2-chlorovinyl adspecies for the adsorption of *cis*-DCE on Pd(1 1 1) has also been proposed by Land and coworkers [16]. The feature near 820 cm^{-1} has been previously assigned as a C–H bending mode for acetylide-like adspecies in the cases of acetylene and ethylene adsorption on Ni(1 0 0) [1,2]. In the present case, the feature located at a similar location (840 cm^{-1}) found for *cis*-DCE and *trans*-DCE (but not for *iso*-DCE) could have additional contribution from the C–Cl stretch in the chlorovinyl adspecies. Although the features at 740 cm^{-1} and 870 cm^{-1} were observed for benzene on the (1 0 0) [5], (1 1 0) [8,22] and (1 1 1) [5] surfaces of Ni, these features were found to be much more intense than the similar features in the present case. The lack of benzene formation in the present case is also in good accord with the observation that the C–H stretch occurs at a lower wavenumber (2860–2910 cm^{-1}) than that found for benzene (>3000 cm^{-1}).

For *iso*-DCE, the better defined EELS features and the very small intensity near 740 cm^{-1} (Fig. 1a) suggest that the dominant adspecies are different from those of its structural isomer homologs, *cis*-DCE (Fig. 1c) and *trans*-DCE (Fig. 1b), on Ni(1 0 0). Based on the aforementioned hypothesis that the dominant surface species are dechlorinated hydrocarbon fragments, a likely candidate for the adsorption of *iso*-DCE on Ni(1 0 0) is the multi-dentate vinylidene-like $(\cdot\dot{C}=CH_2 \leftrightarrow \cdot\ddot{C}-\dot{C}H_2)$ adspecies formed by double dechlorination. Furthermore, the apparent lack of C=C stretch near 1600 cm^{-1} (Fig. 1a) favours the formation of ethylylidyne $(\cdot\ddot{C}-\dot{C}H_2)$ instead of its resonance adspecies, vinylidene $(\cdot\dot{C}=CH_2)$, for *iso*-DCE. The ethylylidyne adspecies has also been observed on many other metal surfaces, including Rh(1 1 1) [23] and Pt(1 1 1) [24] the EELS features of which are also summarized in Table 1. The similar energy positions of the EELS features found for *iso*-DCE on Ni(1 0 0) to those of ethylylidyne observed on Rh(1 1 1) and Pt(1 1 1) are consistent with the formation of ethylylidyne on Ni(1 0 0). On the other hand, unlike DCE on Pd(1 1 1) [16,17], the formation of ethylidyne $(\cdot\ddot{C}-CH_3)$ on Ni(1 0 0) is unlikely, because there is no coordinated sites with three-fold symmetry on the Ni(1 0 0) surface and the repulsive part of the potential dominates in the adsorption sites with fourfold symmetry [25].

In an earlier work, Mate et al. reported that acetylenic and acetylide-like adspecies formed at 77 K on Rh(1 1 1) could be readily converted to ethylylidyne $(\cdot\ddot{C}-\dot{C}H_2)$ above 270 K [23], which would lead to similar EELS signatures for all three DCE isomers. However, this conversion was not observed for acetylenic and acetylide-like adspecies formed at low temperature on Ni(1 0 0) upon warming to RT by Zaera and Hall [1,2], who further concluded that the dehydrogenated hydrocarbon intermediates are very stable and do not rehydrogenate. Other study of acetylene on Ni(1 1 1) by Haug et al. [7] shows that the reaction with surface-bound H is extremely slow, and recombinative H_2 desorption starts to occur at 280 K, further reducing the prospect of rehydrogenation of surface adspecies. Therefore, the conversion of acetylenic and acetylide-like adspecies to ethylylidyne and to ethylidyne in the case of *cis*- and *trans*-DCE and of *iso*-DCE respectively is unlikely, which could give rise to the observed differences in the EELS signatures for *cis*- and *trans*-DCE and for *iso*-DCE on Ni(1 0 0) in the present work.

3.2. Effects of sample annealing

Figs. 2–4 show the EELS spectra of *iso*-, *trans*- and *cis*-DCE adsorbed on Ni(1 0 0) at RT as a function of the flash-annealing temperature, respectively. The samples were annealed to and held at the preset temperatures for 1 min, followed by cooling back to RT before the EELS spectra were recorded. Evidently, dramatic changes in the spectral features for all three DCE isomers are observed. In particular, annealing the *iso*-DCE sample to 350 K (Fig. 2b) substantially reduced the intensities of the three prominent features at 960 cm^{-1}, 1320 cm^{-1} and 2860 cm^{-1}, making the deep valley near 700 cm^{-1} appearing more shallow. The emergence of EELS features at 650 cm^{-1} and 1620 cm^{-1} become more evident with increasing flash-

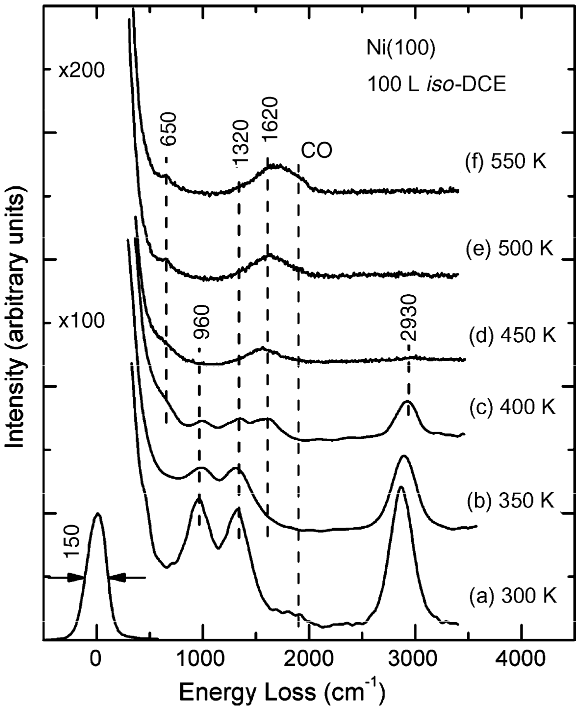

Fig. 2. Electron energy loss spectra of 100 L *iso*-dichloroethylene (DCE) exposed to Ni(1 0 0) (a) at 300 K and upon flash-annealing to (b) 350 K, (c) 400 K, (d) 450 K, (e) 500 K and (f) 550 K.

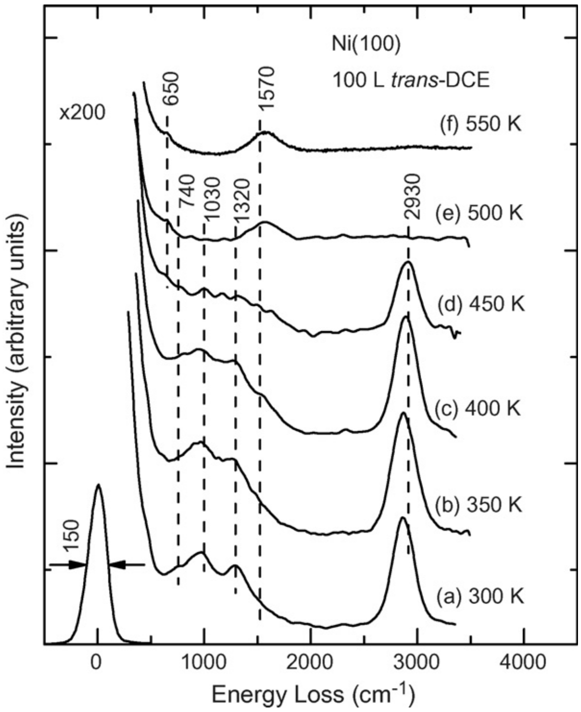

Fig. 3. Electron energy loss spectra of 100 L *trans*-dichloroethylene (DCE) exposed to Ni(1 0 0) (a) at 300 K and upon flash-annealing to (b) 350 K, (c) 400 K, (d) 450 K, (e) 500 K and (f) 550 K.

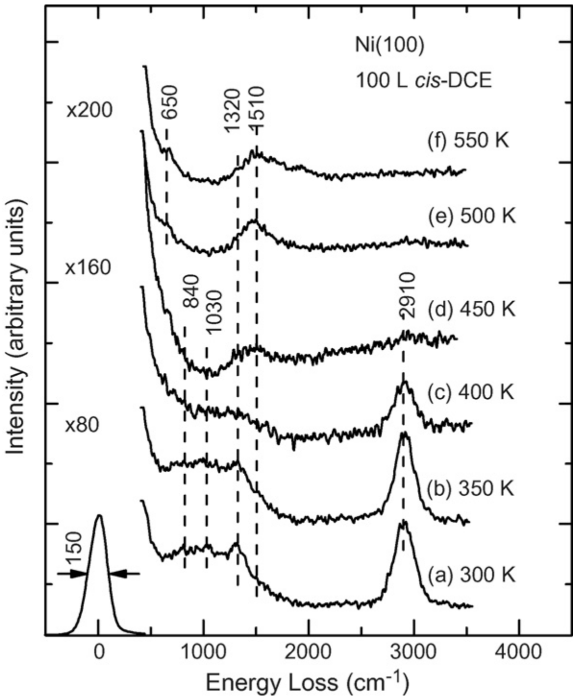

Fig. 4. Electron energy loss spectra of 100 L *cis*-dichloroethylene (DCE) exposed to Ni(1 0 0) (a) at 300 K and upon flash-annealing to (b) 350 K, (c) 400 K, (d) 450 K, (e) 500 K and (f) 550 K.

annealing temperature (400 K, Fig. 2c). These notable changes suggest that the proposed ethylylidyne $(\cdot\ddot{C}-\dot{C}H_2)$ adspecies may undergo dehydrogenation, forming acetylide-like $(\cdot\dot{C}=\dot{C}H \leftrightarrow \cdot\ddot{C}-\ddot{C}H)$ and/or C-containing adspecies. The new features at 650 cm^{-1} and 1620 cm^{-1} could be attributed to, respectively, Ni–C asymmetric stretch [26] and C=C stretch of remaining acetylide-like and carbon cluster adspecies [27]. Furthermore, the C–H stretching mode observed at 2860 cm^{-1} at RT also appears to shift to 2930 cm^{-1} upon further annealing to 400 K. A theoretical study on the thermal evolution of acetylene on Cu(1 0 0) by Yuan et al. [28] showed that the C–H stretching mode occurs at a higher wavenumber for acetylide-like adspecies than ethylylidyne adspecies. Given that the C–H stretch wavenumber for sp^2-hybridized C is generally higher than that for sp^3-hybridized C, the observed blue-shift could also indicate possible conversion of the $\cdot\ddot{C}-\ddot{C}H$ adspecies to the $\cdot\dot{C}=\dot{C}H$ adspecies upon annealing to 400 K. Along with the prominent features at 960 and 1320 cm^{-1}, the feature at 2930 cm^{-1} has essentially disappeared at the annealing temperature of 450 K (Fig. 2d), which indicates complete breakdown of hydrocarbon fragments on the surface. At the same time, the remaining features at 650 and 1620 cm^{-1} appeared to be unaffected at this temperature, and upon further annealing to 550 K (Fig. 2f). The weak peak at 1905 cm^{-1} observed at higher temperature corresponds to C=O stretch due to possible contamination by residual CO in the UHV chamber [19].

Unlike *iso*-DCE, annealing the *trans*-DCE sample to 350 K only caused a minor reduction in the overall spectral features (Fig. 3b), which suggests that the ethylylidyne adspecies found for *iso*-DCE is less stable than the acetylenic and acetylide-like adspecies for *trans*-DCE (and *cis*-DCE). Like *iso*-DCE, further flash-annealing the sample to 400 K caused the C–H stretching mode at 2860 cm^{-1} to undergo a blue-shift to 2930 cm^{-1}, along with the emergence of a weak EELS feature near 1570 cm^{-1}, characteristic of the C=C stretching mode (Fig. 3c). At an annealing temperature of 500 K, almost all the EELS features at 740, 1030, 1320 and 2930 cm^{-1} completely disappear, while the feature near 1570 cm^{-1} becomes more well-defined, along with a second new feature appearing at 650 cm^{-1} (Fig. 3e). The features at 650 and ~1570 cm^{-1} remain unchanged at the higher flash-annealing temperature of 550 K. Essentially the same spectral evolution as a function of the flash-annealing temperature as that for *trans*-DCE (Fig. 3) can be observed for *cis*-DCE on Ni(1 0 0) (Fig. 4). Similar reduction in the intensities of the prominent features at 840, 1030, 1320 and 2910 cm^{-1} upon annealing to 400 K (Fig. 4c) are also found. At 550 K, only the newly emerged EELS features at 650 and 1510 cm^{-1} are found to remain.

Despite the different EELS spectra for the as-deposited samples at RT, the remarkably similar EELS spectra obtained at 550 K for all three DCE isomers suggest that the remaining fragments on the Ni(1 0 0) surface after the 550 K anneal are the same. These fragments could likely be carbon clusters, with the EELS features found near 650 and 1510 cm^{-1} corresponding to the characteristic Ni–C asymmetric stretch and C=C stretch modes, respectively [26,27]. It should be noted that similar TDS data have also been obtained for all three isomers (not shown). These TDS results do not reveal any discernible features attributable to molecular desorption or desorption of fragments related to acetylene, ethylene and/or benzene, though vibrational signatures related to acetylenic adspecies are observed in the corresponding RT EELS spectra. The lack of these hydrocarbon-containing products is consistent with the observation by Zaera and Hall that most of the surface adspecies undergo dissociation on Ni(1 0 0) [1,2]. Recombinative desorption of HCl (*m*/*z* 36) and/or Cl_2 (*m*/*z* 70) has been found to be weak in the TDS experiments, which indicates that

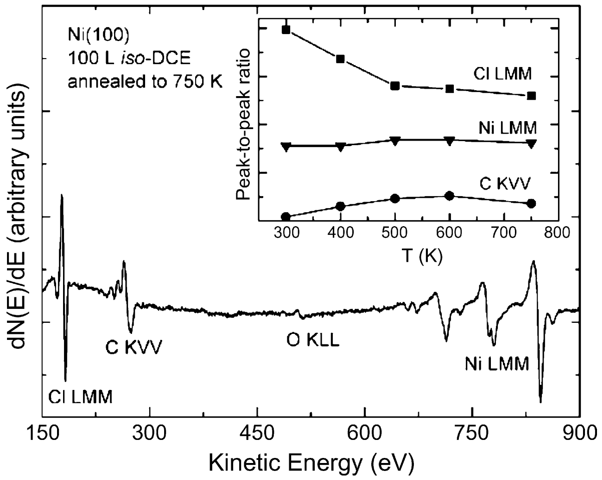

Fig. 5. Auger electron spectrum of 100 L *iso*-dichloroethylene (DCE) exposed to Ni(1 0 0) at room temperature and upon flash-annealing to 750 K. The inset shows the relative peak-to-peak ratios of Cl LMM, C KVV, and Ni LMM Auger lines (arbitrarily normalized to the Ni LMM value at 750 K) as a function of flash-annealing temperature.

most of the dissociated Cl atoms must remain on the Ni(1 0 0) surface after annealing (in contrast to that found on Cu(1 1 0) [12,13]. It should be noted that the Cu surface, unlike the Ni(1 0 0) surface, is not sufficiently reactive to activate the C–H bond breakage, therefore eliminating the source of H atoms required for recombinative HCl desorption. Furthermore, recombinative desorption of H_2 (m/z 2) has been detected at ∼380 K for Ni(1 0 0). Similar thermal evolution behaviours have been observed on Pt surface, on which desorption of HCl at 460 K has also been reported [9].

The nature of the remaining Cl-containing fragments on the Ni(1 0 0) surface can be further examined by AES. Fig. 5 shows a typical AES spectrum of *iso*-DCE adsorbed on Ni(1 0 0) at RT after being flash-annealed up to 750 K, with the inset depicting the corresponding C, Cl and Ni elemental profiles as a function of the flash-annealing temperature. As expected, the relative peak-to-peak ratio of the LMM Auger line at 849 eV of Ni (the substrate) remains essentially flat over the annealing temperature range in the present experiment. Annealing the sample to 500 K introduced a notable reduction in the peak-to-peak ratio of the Cl LMM feature at 181 eV (Fig. 5, inset), which remains unchanged to 750 K. On the other hand, the C KVV signal at 272 eV increases with increasing flash-annealing temperature to 600 K, above which slight reduction occurs, which could due to C diffusion to the near surface below 600 K and back to the bulk above 600 K. These spectral changes suggest reduction in the relative surface concentration of Cl upon annealing to 500 K, consistent with the recombinative HCl desorption observed below 500 K in our TDS experiments. Both TDS and AES results also show that desorption of Cl-containing species on the surface is not significant upon further annealing to 750 K. The small decrease in the C KVV signal above 600 K shows possible carbon diffusion into the bulk. Similar AES experiments have also been performed for the *trans*- and *cis*-DCE isomers and similar results were obtained.

4. Conclusions

In summary, the RT adsorption properties of *cis*- and *trans*-DCE on Ni(1 0 0) have been compared with that of their structural isomer, *iso*-DCE. Both *cis*- and *trans*-DCE exhibit similar vibrational spectra that are discernibly different from that of *iso*-DCE. For *cis*- and *trans*-DCE on Ni(1 0 0), the similarities found for the EELS features to those for acetylene or ethylene adsorption on Ni(1 0 0) strongly suggest the presence of the acetylenic and acetylide-like adspecies. For *iso*-DCE on Ni(1 0 0), the corresponding EELS spectra indicate the presence of ethylylidyne. Thermal evolution of the spectral features for all three isomers are found to be similar, with the emergence of the asymmetric Ni–C stretch at 650 cm^{-1} and C═C stretch at ∼1600 cm^{-1} related to carbon cluster fragments above 500 K. The lack of significant reduction in the Cl LMM Auger line upon further annealing to 750 K illustrates the stabilities of these Cl or Cl-containing adspecies on Ni(1 0 0). The presence of surface Cl appears to prevent the cleavage of C–C bonds and promote the formation of carbon clusters.

Acknowledgement

This work was supported by the Natural Sciences and Engineering Research Council of Canada.

References

[1] F. Zaera, R.B. Hall, J. Phys. Chem. 91 (1987) 4318, and references therein.
[2] F. Zaera, R.B. Hall, Surf. Sci. 180 (1987) 1, and references therein.
[3] C.G.P.M. Bernardo, J.A.N.F. Gomes, J. Mol. Struct. (Theochem.) 542 (2001) 263.
[4] S. Lehwald, H. Ibach, H. Steininger, Surf. Sci. 117 (1982) 342.
[5] J.C. Bertolini, J. Rousseau, Surf. Sci. 89 (1979) 467.
[6] J.A. Stroscio, S.R. Bare, W. Ho, Surf. Sci. 148 (1984) 499.
[7] K.L. Haug, T. Buergi, M. Gostein, T.R. Trautman, S.T. Ceyer, J. Phys. Chem. B 105 (2001) 11480.
[8] D.R. Huntley, S.L. Jordan, F.A. Grimm, J. Phys. Chem. 96 (1992) 1409.
[9] V.H. Grassian, G.C. Pimentel, J. Chem. Phys. 88 (1988) 4478.
[10] A. Cassuto, M.B. Hugenschmidt, P. Parent, C. Laffon, G. Tourillon, Surf. Sci. 310 (1994) 390.
[11] M.X. Yang, P.W. Kash, D.-H. Sun, G.W. Flynn, B.E. Bent, M.T. Holbrook, S.R. Bare, D.A. Fischer, J.L. Gland, Surf. Sci. 380 (1997) 151.
[12] Y. Jugnet, N.S. Prakash, J.C. Bertolini, S.C. Laroze, R. Raval, Catal. Lett. 56 (1998) 17.
[13] S.C. Laroze, S. Haq, R. Raval, Y. Jugnet, J.-C. Bertolini, Surf. Sci. 433–435 (1999) 193.
[14] K.T. Park, K. Klier, C.B. Wang, W.X. Zhang, J. Phys. Chem. B 101 (1997) 5420.
[15] L.H. Bloxham, S. Haq, C. Mitchell, R. Raval, Surf. Sci. 489 (2001) 1.
[16] D.M. Jaramillo, D.E. Hunka, D.P. Land, Langmuir 20 (2004) 5782.
[17] D.E. Hunka, D.C. Herman, K.D. Lormand, D.M. Jaramillo, D.P. Land, Langmuir 21 (2005) 8333.
[18] H. Yu, D.Q. Hu, K.T. Leung, J. Vac. Sci. Technol. A 15 (1997) 2653.
[19] M.A. Chesters, D. Lennon, Surf. Sci. 426 (1999) 92.
[20] D.P. Pursell, M. Bocquet, J.M. Vohs, H. Dai, Surf. Sci. 522 (2003) 90.
[21] J.M. Buriak, Chem. Rev. 102 (2002) 1271.
[22] J.C. Bertolini, J. Massardier, B. Tardy, J. Chim. Phys. 78 (1981) 939.
[23] C.M. Mate, C.-T. Kao, B.E. Bent, G.A. Somorjai, Surf. Sci. 197 (1988) 183.
[24] H. Ibach, S. Lehwald, J. Vac. Technol. 15 (1978) 407.
[25] P.D. Ditlevsen, M.A. Van Hove, G.A. Somorjai, Surf. Sci. 292 (1993) 267.
[26] J.C. Bertolini, B. Tardy, Surf. Sci. 102 (1981) 131.
[27] B.K. Agrawal, S. Agrawal, S. Singh, J. Nanosci. Nanotechnol. 5 (2005) 442, and references therein.
[28] L.F. Yuan, J. Yang, Q. Li, Q.-S. Zhu, J. Chem. Phys. 116 (2002) 3104.